

Multimodal Prototype-Enhanced Network for Few-Shot Action Recognition

Xinzhe Ni¹, Yong Liu¹, Hao Wen¹, Yatai Ji¹, Jing Xiao², Yujiu Yang^{1*}

¹Tsinghua Shenzhen International Graduate School, Tsinghua University ²Ping An Insurance (Group) Company of China
{nxz22, liu-yong20, wenh22, jyt21}@mails.tsinghua.edu.cn, xiaojing661@pingan.com.cn
yang.yujiu@sz.tsinghua.edu.cn

Abstract

Current methods for few-shot action recognition mainly fall into the metric learning framework following ProtoNet, which demonstrates the importance of prototypes. Although they achieve relatively good performance, the effect of multimodal information is ignored, e.g. label texts. In this work, we propose a novel **MultimOdal PRototype-ENhanced Network (MORN)**, which uses the semantic information of label texts as multimodal information to enhance prototypes. A CLIP visual encoder and a frozen CLIP text encoder are introduced to obtain features with good multimodal initialization. Then in the visual flow, visual prototypes are computed by a Temporal-Relational CrossTransformer (TRX) module for example. In the text flow, a semantic-enhanced (SE) module and an inflating operation are used to obtain text prototypes. The final multimodal prototypes are then computed by a multimodal prototype-enhanced (MPE) module. Besides, we define a **PRototype SIMilarity DiffERENCE (PRIDE)** to evaluate the quality of prototypes, which is used to verify our improvement on the prototype level and effectiveness of MORN. We conduct extensive experiments on four popular datasets, and MORN achieves state-of-the-art results on HMDB51, UCF101, Kinetics and SSv2. When plugging PRIDE into the training stage, the performance can be further improved.

Introduction

Few-shot action recognition is a challenging problem in computer vision because of the scarcity of labeled samples and the complicated temporal evolution of videos. Most of the methods (Bishay, Zoumpourlis, and Patras 2019; Kumar Dwivedi et al. 2019; Zhu and Yang 2018; Zhang et al. 2020b; Fu et al. 2020; Cao et al. 2020; Zhang et al. 2020a; Zhang, Zhou, and He 2021; Perrett et al. 2021; Thatipelli et al. 2022; Wang et al. 2022; Huang, Yang, and Sato 2022; Liu et al. 2021; Zhu et al. 2021; Wu et al. 2022) for few-shot action recognition mainly fall into the metric-learning framework, whose key idea is to learn a proper metric space tuned to a particular task. Among various metric-learning works, ProtoNet (Snell, Swersky, and Zemel 2017) has been followed by many works and has far-reaching influence. It proposes Prototype as a representation of each category in a few-shot learning scenario. For the scarcity of samples, it is likely that the overfitting problem will arise with a complicated matching strategy. With prototypes, however, the

model reflects a simpler inductive bias and works better in a limited-data regime, *i.e.* few-shot learning scenario. Since we notice the importance of prototypes, it is natural to ask: *how to obtain representative prototypes?*

Intuitively, it is useful to directly introduce a certain prototype-enhanced module as shown in Figure 1a. Methods with prototype-based strategy (Kumar Dwivedi et al. 2019; Perrett et al. 2021; Zhu et al. 2021) expand the concept of prototype, which is not a simple average of video features. However, the information provided by a single modality is limited especially in the few-shot scenario, and they ignore the effect of multimodal information.

As we know, video is a multimodal carrier rather than a series of RGB images. Multimodal information generally yields better results since different modalities provide complementary information, and is proved by (Huang et al. 2021). Therefore, another strategy is to use multimodal information to obtain a better distance metric as shown in Figure 1b. We select label texts as another modality inspired by ActionCLIP (Wang, Xing, and Liu 2021). There is abundant semantic information in label texts to assist the classification. For example, if one is given several short videos of “lifting up one end of something” without being told what action it is, he may not find the same pattern in a short time. Instead, it is much easier to distinguish them from other actions when knowing the exact label. Based on this fact, we preliminarily combine the semantic information of label texts on the feature level. Compared to unimodal prototype-enhanced strategy in Figure 1a, the model with multimodal feature-enhanced strategy achieves further improvement, which verifies the effectiveness of multimodal information. However, methods with multimodal-based strategy (Zhang et al. 2020b; Fu et al. 2020) ignore the importance of prototypes and only combine the two modalities on the feature level. As a result, there is still room for improvement with multimodal prototype-enhanced strategy.

Considering both prototype and multimodal information, we propose a novel **MultimOdal PRototype-ENhanced Network (MORN)** based on our multimodal prototype-enhanced strategy as shown in Figure 1c. It is simple but well-performed, and can be applied to methods producing prototypes. For example on TRX (Perrett et al. 2021), we firstly obtain visual and text features by a CLIP (Radford et al. 2021) visual encoder and a frozen CLIP text encoder.

*Corresponding author

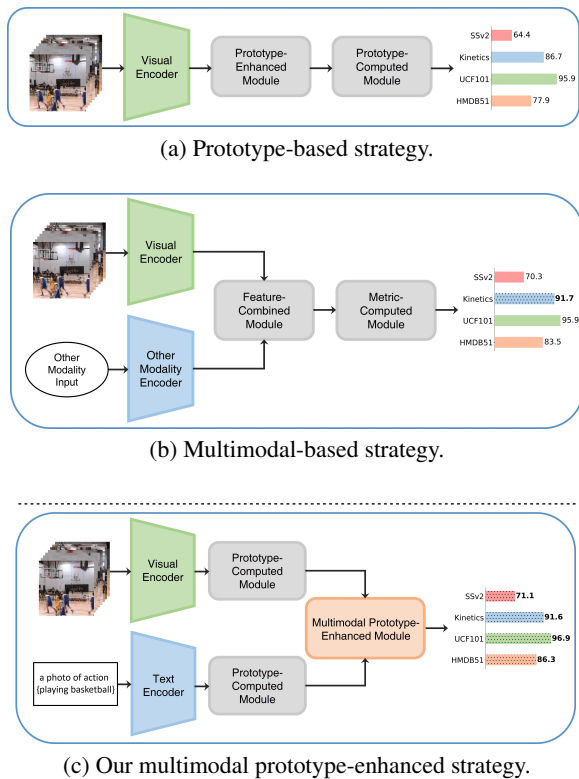


Figure 1: Existing metric-learning strategy (a) and (b) and our multimodal prototype-enhanced strategy (c) for few-shot action recognition. Results on TRX (Perrett et al. 2021) with CLIP visual encoder, multimodal feature-enhanced strategy and multimodal prototype-enhanced strategy are shown.

Then, visual prototypes are computed by TRX baseline, and text prototypes are computed by a semantic-enhanced (SE) module and an inflating operation. Finally, we combine visual prototypes and text prototypes to obtain representative prototypes in a multimodal prototype-enhanced (MPE) module. The final multimodal prototypes are used during the distance computation with query videos. Compared to multimodal feature-enhanced strategy in Figure 1b, MORN achieves better or comparable improvement, which verifies the importance of prototypes.

To verify that our MORN achieves improvement on prototypes rather than other aspects, there is a strong need to evaluate the quality of prototypes with our MORN. Inspired by (Zhang et al. 2021), we define **PR**ototype **SI**milarity **D**ifference (PRIDE). Firstly, we compute the real prototype of each category of all samples in the meta-test stage, and the similarity of current prototypes in an episode with all real prototypes. Then, the difference of similarity between its own category and the average of other categories is used to evaluate the quality of prototypes. With experiments on PRIDE, we are convinced that our MORN achieves improvement on the prototype level. Since PRIDE indicates the quality of prototypes, it can also be used to assist the training process. Therefore, we plug PRIDE into the training stage of MORN and achieve further performance gains.

Our contributions can be summarized as follows:

- We use the semantic information of label texts to enhance prototypes and propose a simple but well-performed Multimodal Prototype-Enhanced Network (MORN).
- We define Prototype Similarity Difference (PRIDE) to verify improvement on the prototype level and effectiveness of MORN. When plugging PRIDE into the training stage, MORN can achieve further performance gains.
- We conduct extensive experiments on four popular action recognition datasets and the application of PRIDE. Methods with MORN achieve state-of-the-art results on HMDB51, UCF101, Kinetics and SSv2.

Related Work

Few-Shot Image Classification

Few-shot image classification methods can be widely divided into three categories: augmentation-based, optimization-based and metric-based.

Augmentation-based methods. The objective of these methods is to use augmentation techniques or extra data to increase samples for training, and improve the diversity of data. Some prior attempts are intuitive, including (Perez and Wang 2017; Ratner et al. 2017). Besides, some works focus on the semantic feature level, including (Chen et al. 2018, 2019). Rather than applying augmentation techniques, (Pahde et al. 2019, 2021) introduce a GAN (Goodfellow et al. 2020) architecture to generate extra images based on the text description to compensate for the lack of data.

Optimization-based methods. The objective of these methods is to train a model under the meta-learning framework so that it can adapt to novel tasks with only a few optimization steps. (Andrychowicz et al. 2016; Gui et al. 2018; Lee et al. 2019; Liu, Schiele, and Sun 2020; Ravi and Larochelle 2017) use the meta-learner as an optimizer. MAML (Finn, Abbeel, and Levine 2017) and its variants (Antoniou, Edwards, and Storkey 2018; Jamal and Qi 2019; Sun et al. 2019) aim to learn a robust model initialization.

Metric-based methods. The objective of these methods is to learn feature embeddings under a certain distance metric with a better generalization ability. Samples of novel categories can be accurately classified via a nearest neighbor classifier with different distance metrics such as cosine similarity (Vinyals et al. 2016; Ye et al. 2020), Euclidean distance (Snell, Swersky, and Zemel 2017; Yoon, Seo, and Moon 2019), non-linear metric with CNNs (Sung et al. 2018; Hou et al. 2019; Li et al. 2019) or graph neural networks (Kim et al. 2019; Garcia and Bruna 2018; Yang et al. 2020). Our work falls into the metric-learning framework and aims to solve a more complicated few-shot video action recognition problem.

Few-Shot Action Recognition

Most of the methods for few-shot action recognition mainly fall into the metric-learning framework. More specifically, we divide them into three categories: feature-based, multimodal-based and prototype-based.

Feature-based methods. The objective of these methods is to obtain reliable video features or apply an effective alignment strategy. CMN (Zhu and Yang 2018), TARN (Bishay, Zoumpourlis, and Patras 2019), OTAM (Cao et al. 2020) and ARN (Zhang et al. 2020a) make preliminary attempts to obtain reliable video features for classification. ITANet (Zhang, Zhou, and He 2021) introduces a video representation based on a self-attention mechanism and an implicit temporal alignment. MASTAF (Liu et al. 2021) uses self-attention and cross-attention mechanisms to obtain reliable spatial-temporal features. MT-FAN (Wu et al. 2022) designs a motion modulator and a segment attention mechanism, and conducts a temporal fragment alignment. STRM (Thatipelli et al. 2022) proposes a local patch-level and a global frame-level enrichment module based on TRX. Similarly, HyRSM (Wang et al. 2022) proposes a hybrid relation module to enrich video features.

Prototype-based methods. Prototype is a representation of each category, and is proposed by ProtoNet (Snell, Swersky, and Zemel 2017). The objective of these methods is to compute representative prototypes by some prototype-enhanced strategies with a single modality. ProtoGAN (Kumar Dwivedi et al. 2019) generates extra samples by using a conditional GAN with category prototypes. PAL (Zhu et al. 2021) matches a prototype with all the query samples instead of matching a query sample with the space of prototypes. TRX (Perrett et al. 2021) applies CrossTransformer (Doersch, Gupta, and Zisserman 2020) to a few-shot action recognition scenario to obtain query-specific category prototypes.

Multimodal-based methods. The objective of these methods is to use multimodal information to assist classification. AMeFu-Net (Fu et al. 2020) introduces depth information as another modality to assist classification. CMMN (Zhang et al. 2020b) also uses the semantic information of label texts as ours and is similar to our multimodal setting. However, it fails to apply a feature extractor with a good multimodal initialization and ignores the importance of prototypes. CPMT (Huang, Yang, and Sato 2022) uses object features as multimodal information and proposes a compound prototype-matching strategy. Thus, CPMT can be regarded as a multimodal-based method with a prototype-based design. Our work also uses multimodal information and further computes representative prototypes. Furthermore, we notice the remarkable effect of the semantic information of label texts and the prototype-enhanced strategy.

Method

Problem formulation

There are two sets in the N -way K -shot few-shot scenario: a support set $S_K^N = \{s_1^1, \dots, s_K^1, \dots, s_1^N, \dots, s_K^N\}$ and a query set $Q_M^N = \{q_1^1, \dots, q_M^1, \dots, q_1^N, \dots, q_M^N\}$, where N denotes the number of different action categories, K denotes the number of videos each category in the support set and M denotes the number of videos each category in the query set. The objective of few-shot action recognition is to learn a model with great generalization ability using only a few video samples. Specifically, the model classifies a completely novel query action to the right category by

matching it with the most similar video in the support set. Meanwhile, the whole dataset is divided into a base dataset $C_{base} = \{(x_i, y_i)\}_{i=1}^{|C_{base}|}$ and a novel dataset $C_{novel} = \{(x_i, y_i)\}_{i=1}^{|C_{novel}|}$, where y_i is the action category of a video sample x_i . Note that the categories of C_{base} and C_{novel} are label-wise non-overlapping, *i.e.* $C_{base} \cap C_{novel} = \emptyset$. To make full use of the few video samples, we follow the episode training manner (Vinyals et al. 2016). Each episode contains K videos in the support set and M videos in the query set of N categories.

MORN

Considering both prototype and multimodal information, we propose MORN. The overall architecture is shown in Figure 2, including a visual flow, a text flow and a multimodal prototype-enhanced (MPE) module.

Visual flow. For each input video, we uniformly sample L frames as in (Wang et al. 2016). The video s_k^n in the support set and q_m^n in the query set can be further denoted as:

$$\begin{aligned} s_k^n &= \{s_{k1}^n, \dots, s_{kL}^n\}, \\ q_m^n &= \{q_{m1}^n, \dots, q_{mL}^n\}, \end{aligned} \quad (1)$$

where $s_k^n, q_m^n \in \mathbb{R}^{L \times H \times W \times 3}$. H and W denote the height and width of an image. Then, we apply a pre-trained CLIP visual encoder for better multimodal initialization. The visual features of each frame $s_{ki}^n \in \mathbb{R}^{H \times W \times 3}$ in the support set and $q_{mi}^n \in \mathbb{R}^{H \times W \times 3}$ in the query set are defined as:

$$\begin{aligned} F_{sk}^V &= \{f_v(s_{k1}^n), \dots, f_v(s_{kL}^n)\}, \\ F_{qm}^V &= \{f_v(q_{m1}^n), \dots, f_v(q_{mL}^n)\}, \end{aligned} \quad (2)$$

where $F_{sk}^V, F_{qm}^V \in \mathbb{R}^{L \times d}$. The visual features of videos in the support set and the query set are denoted as:

$$\begin{aligned} F_s^V &= \{F_{s1}^V, \dots, F_{s(NK)}^V\}, \\ F_q^V &= \{F_{q1}^V, \dots, F_{q(NM)}^V\}, \end{aligned} \quad (3)$$

where $F_s^V \in \mathbb{R}^{NK \times L \times d}$ and $F_q^V \in \mathbb{R}^{NM \times L \times d}$. Then, we sample tuples of video frames $F_q^{Tupl} = \{F_{q1}^{Tupl}, \dots, F_{q(NM)}^{Tupl}\}$ and compute visual prototypes of each episode through TRX:

$$P^V = TRX(F_q^V, F_s^V, F_s^V), \quad (4)$$

where $F_q^{Tupl}, P^V \in \mathbb{R}^{NM \times C_L^\omega \times d_p}$, and C_L^ω is the combinatorial number.

Text flow. In the training stage for each sample $(x_i, y_i) \in C_{base}$, we firstly make n_{temp} discrete templates $P_{temp} = \{p_1^{temp}, \dots, p_{n_{temp}}^{temp}\}$ of y_i as text prompts. Then, we apply a CLIP text tokenizer to obtain tokenized text sequences T_i :

$$\begin{aligned} T_i &= Tokenizer(p_j^{temp} || y_i), \\ j &= 1, \dots, n_{temp}, i = 1, \dots, N, \end{aligned} \quad (5)$$

where $||$ denotes a concatenation operation. In the practical meta-training and meta-test stage, the template is randomly

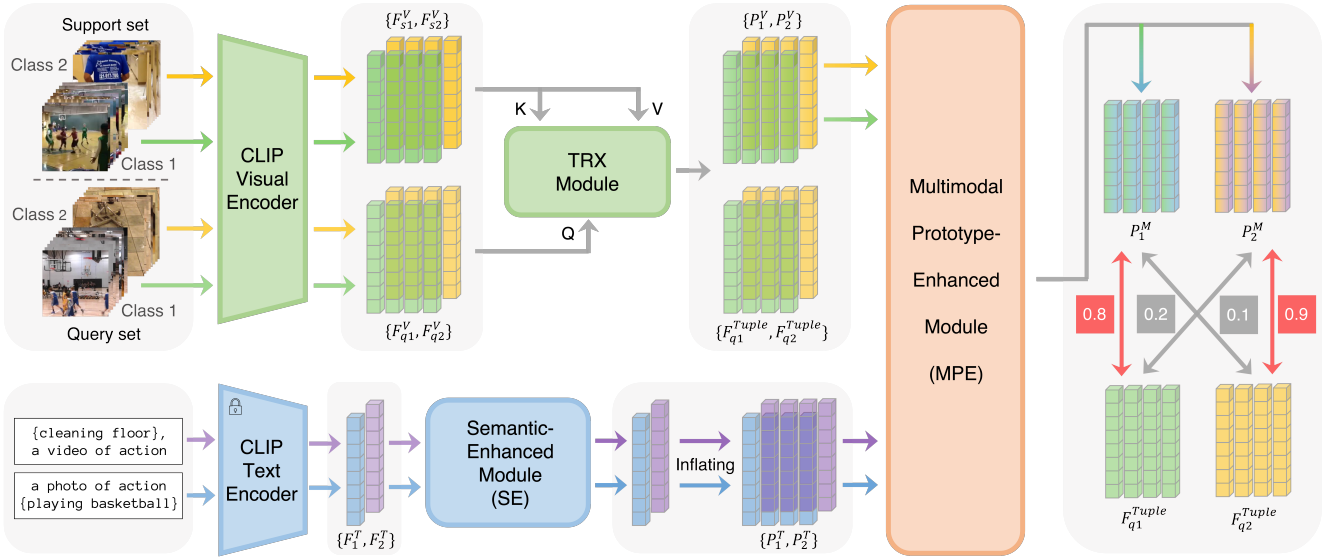


Figure 2: Overview of our proposed MORN on TRX on a 2-way 1-shot problem with 1 video for each category in the query set. In the visual flow, a CLIP visual encoder is first introduced on videos with L frames to obtain video features. Then, support video features are passed to the Temporal-Relational CrossTransformer (TRX) module to compute visual prototypes. In the text flow, a frozen CLIP text encoder is first introduced on the prompted label texts. Then, the semantic features of label texts are passed to a semantic-enhanced (SE) module and are inflated as text prototypes. The visual prototypes and the text prototypes are combined through a multimodal prototype-enhanced (MPE) module.

selected once per episode. Then, the features of prompted label texts are obtained by a frozen CLIP text encoder:

$$F_i^T = f_t(T_i), \{i | x_i \in S_K^N \cup Q_M^N\}, \quad (6)$$

where $F_i^T \in \mathbb{R}^{1 \times d}$. To obtain text features with more reliable semantic information, we further apply a semantic-enhanced (SE) module $g(\cdot)$:

$$P_i^T = g(F_i^T), \quad (7)$$

where $P_i^T \in \mathbb{R}^{1 \times d_p}$ and a multi-head attention mechanism with 4 heads is used as $g(\cdot)$. So we obtain $\{P_1^T, \dots, P_{NM}^T\}$ in each episode. Since different frames of videos in the same category have the same label, we simply inflate P_i^T of the same category to keep the same dimension with visual prototypes. Then, we obtain text prototypes P^T :

$$P^T = \{P_1^T, \dots, P_1^T, \dots, P_N^T, \dots, P_N^T\}, \quad (8)$$

where $P^T \in \mathbb{R}^{NM \times C_L^\omega \times d_p}$.

Multimodal prototype-enhanced module. To use multimodal information to enhance prototypes, we propose a simple but well-performed multimodal prototype-enhanced (MPE) module. The choice of the MPE module is flexible containing weighted average, multi-head attention and so on. Here, we apply weighted average as our default setting:

$$P^M = (1 - \lambda)P^V + \lambda P^T, \quad (9)$$

where $P^M \in \mathbb{R}^{NM \times C_L^\omega \times d_p}$ and λ is the multimodal enhanced hyper-parameter. The multimodal prototypes are used as the final prototypes. Then, distances are computed between multimodal prototypes and F_q^{Tuple} , and are passed as logits to a cross-entropy loss.

PRIDE

Denote the number of categories in the meta-test stage as N_{novel} . We first compute the real prototype in a 1-way scenario by averaging all prototypes of the same category i in the novel dataset, which is based on (Zheng et al. 2021):

$$P_i^{real} = \frac{1}{|C_{novel}^i|} \sum_{(x,y) \in C_{novel}^i} P_i(x), \quad (10)$$

where $P_i(x)$ is the query-specific category prototype of video x and C_{novel}^i is the i -th category in C_{novel} . The whole set of real prototypes is denoted as:

$$P^{real} = \{P_1^{real}, \dots, P_{N_{novel}}^{real}\}. \quad (11)$$

Then, the cosine similarity can be computed between a given $P_i(x)$ and P_j^{real} :

$$Sim_j = sim(P_i(x), P_j^{real}), j = 1, \dots, N_{novel}, \quad (12)$$

where $sim(\cdot, \cdot)$ is the cosine similarity operation. The similarity of other categories is denoted as:

$$Sim_{other} = \frac{1}{N_{novel} - 1} \sum_{1 \leq j \neq i \leq N_{novel}} Sim_j. \quad (13)$$

We can now denote PRIDE as:

$$PRIDE_i(x) = Sim_i - Sim_{other}, (x, y) \in C_{novel}^i. \quad (14)$$

According to the computation process, PRIDE can accurately reflect the category separability of prototypes. Thus, PRIDE can be used to verify the improvement on the prototype level and the effectiveness of our MORN. A higher PRIDE value means more representative prototypes with a better discriminating ability.

Method	Strategy	Backbone	HMDB51	UCF101	Kinetics	SSv2	Average
ARN (Zhang et al. 2020a)	Feature-based	C3D	60.6	83.1	82.4	-	75.4
OTAM (Cao et al. 2020)		ResNet-50	68.0	88.9	85.8	52.3	73.8
HyRSM (Wang et al. 2022)			76.0	94.7	86.1	69.0	81.5
MT-FAN (Wu et al. 2022)			74.6	95.1	87.4	60.4	79.4
STRM (Thatipelli et al. 2022)			77.3	<u>96.9</u>	86.7	68.1	82.3
PAL (Zhu et al. 2021)	Prototype-based	ResNet-50	75.8	95.2	87.1	62.6	80.2
TRX (Perrett et al. 2021)			75.6	96.1	85.9	64.6	80.6
CMMN (Zhang et al. 2020b)	Multimodal-based	C3D + MLP	70.5	87.7	-	-	79.1
AMeFu-Net (Fu et al. 2020)		ResNet-50 + ResNet-50	75.5	95.5	86.8	-	85.9
CPMT (Huang, Yang, and Sato 2022)		ResNet-50 + Mask-RCNN	85.1	92.3	87.9	<u>73.5</u>	84.7
Ours: STRM ^M (Weighted average)	Prototype-based & Multimodal-based	CLIP ResNet-50 + CLIP text encoder	84.4	94.6	90.5	73.6	85.8
Ours: TRX ^M (Weighted average)			<u>86.3</u>	<u>96.9</u>	91.6	71.1	86.5
Ours: STRM ^M (Multi-head Attention)			86.2	96.4	<u>93.8</u>	71.9	<u>87.1</u>
Ours: TRX ^M (Multi-head Attention)			87.1	97.7	94.6	71.7	87.8

Table 1: State-of-the-art comparison on four few-shot action recognition datasets in terms of classification accuracy. “Weighted average” and “Multi-head Attention” denotes different choices of the MPE module. *^M denotes methods with our MORN. The bold font and underline indicate the best and second-best results respectively.

Experiments

Datasets. We evaluate our method on four popular datasets: HMDB51 (Kuehne et al. 2011), UCF101 (Soomro, Zamir, and Shah 2012), Kinetics (Carreira and Zisserman 2017) and Something-Something V2 (SSv2) (Goyal et al. 2017). HMDB51 contains 51 action categories, each containing at least 101 clips for a total of 6,766 video clips. For HMDB51, we adopt the same protocol as (Zhang et al. 2020a) with 31/10/10 categories for train/val/test. UCF101 contains 101 action categories, each containing at least 100 clips for a total of 13,320 video clips. For UCF101, we also adopt the same protocol as (Zhang et al. 2020a) with 70/10/21 categories for train/val/test. Kinetics contains 400 action categories with 400 or more clips for each category. For Kinetics, we adopt the same protocol as (Zhu and Yang 2018) with 64/12/24 categories for train/val/test. SSv2 contains 220,847 videos of fine-grained actions with only subtle differences between categories, and is regarded as a more challenging task. For SSv2, we adopt the same protocol as (Cao et al. 2020) with 64/12/24 categories for train/val/test.

Baseline. Our work adopts STRM (Thatipelli et al. 2022) and TRX (Perrett et al. 2021) as baseline. STRM is a feature-based method based on TRX, and TRX applies CrossTransformer (Doersch, Gupta, and Zisserman 2020) to the few-shot action recognition scenario. CrossTransformer combines the information of support images and query images through an attention operation. TRX further samples ordered sub-sequences of video frames called tuples, and thus can capture higher-order temporal relationships.

Comparison with State-of-the-arts

As shown in Table 1, we apply MORN on STRM (Thatipelli et al. 2022) and TRX (Perrett et al. 2021), and comprehensively compare four datasets for the standard 5-way 5-shot action recognition task with state-of-the-art methods. CPMT (Huang, Yang, and Sato 2022) uses both object features and a compound prototype-matching strategy, thus achieves the best results before us on HMDB51, Kinetics

Method	HMDB51	UCF101	Kinetics	SSv2
STRM ^C	10.0	17.5	16.5	8.6
Ours: STRM ^M	17.1	23.5	26.5	48.2
TRX ^C	7.4	15.3	16.4	10.4
Ours: TRX ^M	17.4	24.4	26.9	47.3

Table 2: Average PRIDE values across prototypes computed in C_{novel} on HMDB51, UCF101, Kinetics and SSv2. *^C denotes methods with CLIP visual encoder.

and SSv2. Compared to CPMT, our MORN achieves the best results of 87.1%, 97.7%, 94.6% and 73.6% on all four datasets. Also, there is significant improvement over STRM and TRX baseline with our MORN. When using weighted average as MPE module, STRM^M achieves performance gains of 7.1% on HMDB51, 3.8% on Kinetics and 5.5% on SSv2 over STRM, and TRX^M also achieves similar performance gains. The improvement demonstrates the effectiveness of our multimodal prototype-enhanced strategy.

To further improve the performance of MORN, we use a multi-head attention mechanism with 8 heads as MPE module. With a better MPE, the performance on HMDB51, UCF101 and Kinetics can be further improved, while the performance of STRM^M on SSv2 declines on the contrary. It is probably because some label texts in SSv2 are so similar that it is hard to capture the useful semantic information, e.g. *pouring something into something* against *pouring something onto something*. Plus, we notice the importance of multimodal initialization and introduce CLIP encoders. A more detailed ablation study of the MPE module and encoders will be illustrated in Section Ablation Study. In summary, MORN achieves the best results of 87.1% and 87.8% with multi-head attention on average. For simplicity and fewer parameters, we apply TRX^M with weighted average as our default setting of MORN.

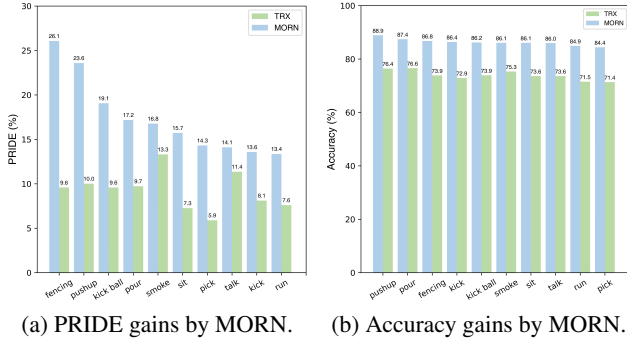


Figure 3: Performance gains and correlation analysis of PRIDE and accuracy on HMDB51. MORN achieves PRIDE gains in (a) and accuracy gains in (b) in each category.

Method	HMDB51	UCF101	Kinetics	SSv2
STRM ^M	84.4	94.6	90.5	73.6
STRM ^{MP}	85.5	95.6	91.2	73.9
TRX ^M	86.3	96.9	91.6	71.1
TRX ^{MP}	86.4	96.9	91.9	72.6

Table 3: *^{MP} denotes methods with our MORN and PRIDE loss. Plugging PRIDE into the training stage of MORN achieves further performance gains, which verifies the rationality of PRIDE and the effectiveness of our MORN.

Multimodal Prototype-Enhanced Analysis

In this subsection, we explore the performance of our multimodal prototype-enhanced strategy. As mentioned earlier, we use PRIDE to evaluate the quality of prototypes. Firstly, we compute PRIDE and verify the effectiveness of our MORN. Furthermore, we plug PRIDE into the training stage of MORN and achieve further performance gains.

Firstly, we randomly sample 10000 test episodes to compute accuracy and PRIDE. As shown in Figure 3a and 3b, MORN achieves significant gains on both PRIDE and accuracy on each category of HMDB51. Then, we conduct experiments of average PRIDE on all four datasets to verify the effectiveness of MORN. For a fair comparison, we replace the original ResNet-50 in TRX and STRM with a CLIP ResNet-50. As shown in Table 2, there is significant improvement of STRM^M and TRX^M on PRIDE over STRM and TRX baseline. Specifically, STRM^M achieves performance gains of 7.1% on HMDB51, 6.0% on UCF101, 10.0% on Kinetics and 39.6% on SSv2 over STRM, and TRX^M also achieves similar PRIDE gains. Note that the improvement on SSv2 is particularly significant because the label texts in SSv2 are more complicated with more semantic information. According to the computation process, PRIDE can accurately reflect the category separability of prototypes. With MORN, we obtain higher PRIDE values over STRM and TRX. It turns out that MORN can improve the quality of prototypes, which verifies the effectiveness of MORN.

To further explore the function of PRIDE, we plug it into

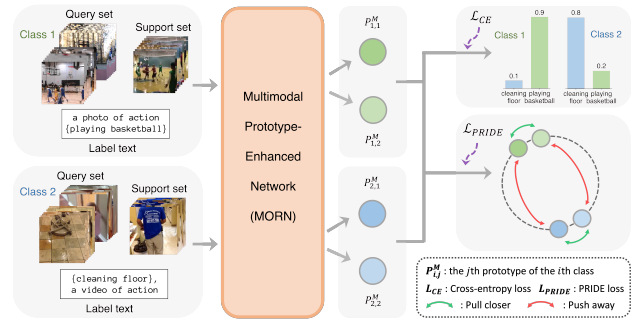


Figure 4: Overview of our proposed MORN with PRIDE loss on a 2-way 1-shot problem with 2 videos for each category in the query set. CE loss and PRIDE loss are combined through a learnable weight.

Method	Backbone	HMDB51	UCF101	Kinetics	SSv2
STRM	ResNet-50	77.3	96.9	86.7	68.1
TRX		75.6	96.1	85.9	64.6
STRM ^C	CLIP ResNet-50	79.3	94.7	86.0	62.9
TRX ^C		77.9	95.9	86.7	64.4
STRM ^{RB}	ResNet-50 + BERT	73.4	94.8	83.2	59.3
TRX ^{RB}		72.0	95.2	83.4	58.8
STRM ^M	CLIP ResNet-50 +	84.4	94.6	90.5	73.6
TRX ^M	CLIP text encoder	86.3	96.9	91.6	71.1

Table 4: Ablation study of various encoders on HMDB51, UCF101, Kinetics and SSv2. *^{RB} denotes methods with ResNet-50 and BERT-large. MORN achieves significant gains with a good multimodal initialization.

the training stage of MORN as a loss as shown in Figure 4. PRIDE loss is implemented through InfoNCE (Oord, Li, and Vinyals 2018) with prototypes:

$$\mathcal{L}_{PRIDE} = -\log \frac{\exp(P_i(x) \cdot P_i^{real} / \tau)}{\sum_{j=1}^{N_{novel}} \exp(P_i(x) \cdot P_j^{real} / \tau)}. \quad (15)$$

We aim at increasing the similarity of prototypes in the same category and decreasing that of prototypes in different categories. CE loss and PRIDE loss are combined through a learnable weight. Since PRIDE indicates the quality of prototypes, it is supposed to assist the training process. In Table 3, STRM^{MP} and TRX^{MP} achieve extra performance gains over STRM^M and TRX^M. The results verify both the rationality of PRIDE and the effectiveness of our MORN.

Ablation Study

Multimodal encoders. We employ label texts as an extra modality, and an intuitive idea is to use BERT (Devlin et al. 2019) as the text encoder. However, the performance of STRM^{RB} and TRX^{RB} declines a lot as shown in Table 4. We refer it to an inadequate multimodal initialization. To verify this, we introduce CLIP encoders with a good multimodal initialization and our prototype-enhanced strategy. STRM^M and TRX^M achieve best results and significantly outperform STRM^{RB} and TRX^{RB}. Furthermore, to verify

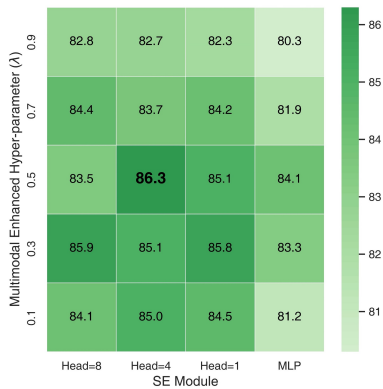


Figure 5: Ablation study of varying the SE module and multimodal enhanced hyper-parameter (λ) on HMDB51.

MPE module	HMDB51	UCF101	Kinetics	SSv2
Concat + MLP	62.0	79.9	76.6	58.3
MLP + Concat	72.4	86.3	80.5	60.6
Weighted average	<u>86.3</u>	<u>96.9</u>	91.6	71.1
Head = 1	81.0	95.5	91.8	72.6
Head = 4	85.1	<u>96.9</u>	<u>94.1</u>	70.3
Head = 8	87.1	97.7	94.6	<u>71.7</u>

Table 5: Ablation study of the MPE module on HMDB51, UCF101, Kinetics and SSv2. ‘‘Concat’’ indicates a concatenation operation and ‘‘Head’’ indicates the head number in multi-head attention mechanism. The bold font and underline indicate the best and second-best results respectively.

the importance of the text flow, we only replace the original ResNet-50 with a CLIP ResNet-50 and obtain STRM^C and TRX^C. The performance varies on four datasets, and is worse than that of STRM^M and TRX^M, demonstrating the importance of multimodal information. In addition, we show the advantage of prototype-enhanced strategy over feature-enhanced strategy in Figure 1. Combining the two aspects, the necessity and effectiveness of our MORN are verified.

Design choices. As shown in Figure 5, we compare various choices of the SE module and multimodal enhanced hyper-parameter (λ) on HMDB51. When using a two-layer MLP with a 1024-dimensional hidden layer, we obtain a low accuracy. It is mainly because MLP has a simple architecture and thus fails to fully explore the semantic information of label texts. Therefore, we focus on the multi-head attention mechanism (Vaswani et al. 2017). As the head number increases, the fitting ability of the SE module improves as well. However, the accuracy fluctuates with different head numbers and λ choices. We need to balance the trade-off between head numbers and λ choices. According to our results, we use a multi-head attention mechanism with 4 heads as the SE module and set λ as 0.5 in our further experiments.

For the MPE module, applying a multi-head attention mechanism can further improve the performance of MORN as shown in Table 5. It turns out that the multimodal information can further enhance the prototypes with a bet-

SE module (exist or not)	CLIP text encoder (freeze or not)	HMDB51	UCF101	Kinetics	SSv2
✗	✗	84.5	96.1	88.8	72.5
✗	✓	83.9	96.4	90.6	72.8
✓	✗	76.7	93.2	87.2	62.1
✓	✓	86.3	96.9	91.6	71.1

Table 6: Ablation study of the SE module and CLIP text encoder on HMDB51, UCF101, Kinetics and SSv2.

ter multimodal combination strategy. MORN achieves the best results with 8 heads on HMDB51, UCF101 and Kinetics, while with 1 head on SSv2. Although weighted average is relatively simple with no parameters for training, our MORN with weighted average can also achieve the second-best results of 86.3% on HMDB51 and 96.9% on UCF101, which has already outperformed those of prior methods. For simplicity and fewer parameters for training, we use weighted average as our default MPE module.

SE module and CLIP text encoder. In the text flow, we first introduce a frozen CLIP text encoder. Then, a semantic-enhanced (SE) module is used to enhance the semantic information. Firstly on SSv2, MORN with a frozen CLIP text encoder is enough to achieve the best result of 72.8% as shown in Table 6. When coming to HMDB51, UCF101 and Kinetics, an SE module further achieves performance gains, and MORN with the SE module and a frozen CLIP text encoder achieves the best results. On the one hand, the function of the SE module is similar to that of the enrichment module in (Thatipelli et al. 2022) to obtain reliable semantic information. On the other hand, a frozen language encoder is proven to be effective in several works (Tsimpoukelli et al. 2021; Rao et al. 2022) and our results further prove it. When we remove the SE module, the results are lower than MORN whether we freeze the CLIP text encoder or not. Besides, using the SE module and fine-tuning the CLIP text encoder leads to the lowest results on all three datasets. It is mainly because the overfitting problem becomes more serious as parameters increase. When coming to SSv2, MORN with a frozen CLIP text encoder but without the SE module achieves the best result. In general, MORN achieves significant performance gains with our design.

Conclusion

We propose a novel Multimodal Prototype-Enhanced Network (MORN) for few-shot action recognition. Our MORN uses the semantic information of label texts as multimodal information to compute more representative prototypes, and achieves state-of-the-art results. We also define Prototype Similarity Difference (PRIDE) to evaluate the quality of prototypes. By conducting experiments on PRIDE, we verify our improvement on prototypes. Besides, plugging PRIDE into the training stage of MORN can achieve further performance gains, verifying the rationality of PRIDE and the importance of prototypes. In summary, we’d like to shed light on a view: *multimodal prototypes with high quality are extremely important in few-shot action recognition.*

References

- Andrychowicz, M.; Denil, M.; Gomez, S.; Hoffman, M. W.; Pfau, D.; Schaul, T.; Shillingford, B.; and De Freitas, N. 2016. Learning to learn by gradient descent by gradient descent. In *NIPS*, volume 29.
- Antoniou, A.; Edwards, H.; and Storkey, A. 2018. How to train your MAML. In *ICLR*.
- Bishay, M.; Zoumpourlis, G.; and Patras, I. 2019. Tarn: Temporal attentive relation network for few-shot and zero-shot action recognition. In *BMVC*, 154.
- Cao, K.; Ji, J.; Cao, Z.; Chang, C.-Y.; and Niebles, J. C. 2020. Few-shot video classification via temporal alignment. In *CVPR*, 10618–10627.
- Carreira, J.; and Zisserman, A. 2017. Quo vadis, action recognition? a new model and the kinetics dataset. In *CVPR*, 6299–6308.
- Chen, Z.; Fu, Y.; Zhang, Y.; Jiang, Y.-G.; Xue, X.; and Sigal, L. 2018. Semantic feature augmentation in few-shot learning. *arXiv preprint arXiv:1804.05298*, 86(89): 2.
- Chen, Z.; Fu, Y.; Zhang, Y.; Jiang, Y.-G.; Xue, X.; and Sigal, L. 2019. Multi-level semantic feature augmentation for one-shot learning. *IEEE Transactions on Image Processing*, 28(9): 4594–4605.
- Devlin, J.; Chang, M.-W.; Lee, K.; and Toutanova, K. 2019. Bert: Pre-training of deep bidirectional transformers for language understanding. In *NAACL-HLT*, volume 1, 4171–4186.
- Doersch, C.; Gupta, A.; and Zisserman, A. 2020. Crosstransformers: spatially-aware few-shot transfer. In *NIPS*, volume 33, 21981–21993.
- Finn, C.; Abbeel, P.; and Levine, S. 2017. Model-agnostic meta-learning for fast adaptation of deep networks. In *ICML*, 1126–1135.
- Fu, Y.; Zhang, L.; Wang, J.; Fu, Y.; and Jiang, Y.-G. 2020. Depth guided adaptive meta-fusion network for few-shot video recognition. In *ACMMM*, 1142–1151.
- Garcia, V.; and Bruna, J. 2018. Few-shot learning with graph neural networks. In *ICLR*.
- Goodfellow, I.; Pouget-Abadie, J.; Mirza, M.; Xu, B.; Warde-Farley, D.; Ozair, S.; Courville, A.; and Bengio, Y. 2020. Generative adversarial networks. *Communications of the ACM*, 63(11): 139–144.
- Goyal, R.; Ebrahimi Kahou, S.; Michalski, V.; Materzynska, J.; Westphal, S.; Kim, H.; Haenel, V.; Fruend, I.; Yianilos, P.; Mueller-Freitag, M.; et al. 2017. The” something something” video database for learning and evaluating visual common sense. In *ICCV*, 5842–5850.
- Gui, L.; Wang, Y.; Ramanan, D.; and Moura, J. M. 2018. Few-shot human motion prediction via meta-learning. In *ECCV*, 432–450.
- Hou, R.; Chang, H.; Ma, B.; Shan, S.; and Chen, X. 2019. Cross attention network for few-shot classification. In *NIPS*, volume 32.
- Huang, Y.; Du, C.; Xue, Z.; Chen, X.; Zhao, H.; and Huang, L. 2021. What makes multi-modal learning better than single (provably). In *NIPS*, volume 34, 10944–10956.
- Huang, Y.; Yang, L.; and Sato, Y. 2022. Compound Prototype Matching for Few-shot Action Recognition. In *ECCV*.
- Jamal, M. A.; and Qi, G.-J. 2019. Task agnostic meta-learning for few-shot learning. In *CVPR*, 11719–11727.
- Kim, J.; Kim, T.; Kim, S.; and Yoo, C. D. 2019. Edge-labeling graph neural network for few-shot learning. In *CVPR*, 11–20.
- Kuehne, H.; Jhuang, H.; Garrote, E.; Poggio, T.; and Serre, T. 2011. HMDB: a large video database for human motion recognition. In *ICCV*, 2556–2563.
- Kumar Dwivedi, S.; Gupta, V.; Mitra, R.; Ahmed, S.; and Jain, A. 2019. Protogan: Towards few shot learning for action recognition. In *CVPRW*.
- Lee, K.; Maji, S.; Ravichandran, A.; and Soatto, S. 2019. Meta-learning with differentiable convex optimization. In *CVPR*, 10657–10665.
- Li, H.; Eigen, D.; Dodge, S.; Zeiler, M.; and Wang, X. 2019. Finding task-relevant features for few-shot learning by category traversal. In *CVPR*, 1–10.
- Liu, R.; Zhang, H.; Pirsiavash, H.; and Liu, X. 2021. MASTAF: A Spatio-Temporal Attention Fusion Network for Few-shot Video Classification. *arXiv preprint arXiv:2112.04585*.
- Liu, Y.; Schiele, B.; and Sun, Q. 2020. An ensemble of epoch-wise empirical bayes for few-shot learning. In *ECCV*, 404–421.
- Oord, A. v. d.; Li, Y.; and Vinyals, O. 2018. Representation learning with contrastive predictive coding. *arXiv preprint arXiv:1807.03748*.
- Pahde, F.; Ostapenko, O.; Hnichen, P. J.; Klein, T.; and Nabi, M. 2019. Self-paced adversarial training for multimodal few-shot learning. In *WACV*, 218–226.
- Pahde, F.; Puscas, M.; Klein, T.; and Nabi, M. 2021. Multimodal prototypical networks for few-shot learning. In *WACV*, 2644–2653.
- Perez, L.; and Wang, J. 2017. The effectiveness of data augmentation in image classification using deep learning. *arXiv preprint arXiv:1712.04621*.
- Perrett, T.; Masullo, A.; Burghardt, T.; Mirmehdi, M.; and Damen, D. 2021. Temporal-relational crosstransformers for few-shot action recognition. In *CVPR*, 475–484.
- Radford, A.; Kim, J. W.; Hallacy, C.; Ramesh, A.; Goh, G.; Agarwal, S.; Sastry, G.; Askell, A.; Mishkin, P.; Clark, J.; et al. 2021. Learning transferable visual models from natural language supervision. In *ICML*, 8748–8763.
- Rao, Y.; Zhao, W.; Chen, G.; Tang, Y.; Zhu, Z.; Huang, G.; Zhou, J.; and Lu, J. 2022. Denseclip: Language-guided dense prediction with context-aware prompting. In *CVPR*, 18082–18091.
- Ratner, A. J.; Ehrenberg, H.; Hussain, Z.; Dunnmon, J.; and Ré, C. 2017. Learning to compose domain-specific transformations for data augmentation. In *NIPS*, volume 30.
- Ravi, S.; and Larochelle, H. 2017. Optimization as a model for few-shot learning. In *ICLR*.

- Snell, J.; Swersky, K.; and Zemel, R. 2017. Prototypical networks for few-shot learning. In *NIPS*, volume 30.
- Soomro, K.; Zamir, A. R.; and Shah, M. 2012. UCF101: A dataset of 101 human actions classes from videos in the wild. *arXiv preprint arXiv:1212.0402*.
- Sun, Q.; Liu, Y.; Chua, T.-S.; and Schiele, B. 2019. Meta-transfer learning for few-shot learning. In *CVPR*, 403–412.
- Sung, F.; Yang, Y.; Zhang, L.; Xiang, T.; Torr, P. H.; and Hospedales, T. M. 2018. Learning to compare: Relation network for few-shot learning. In *CVPR*, 1199–1208.
- Thatipelli, A.; Narayan, S.; Khan, S.; Anwer, R. M.; Khan, F. S.; and Ghanem, B. 2022. Spatio-temporal relation modeling for few-shot action recognition. In *CVPR*, 19958–19967.
- Tsimpoukelli, M.; Menick, J. L.; Cabi, S.; Eslami, S.; Vinyals, O.; and Hill, F. 2021. Multimodal few-shot learning with frozen language models. In *NIPS*, volume 34, 200–212.
- Vaswani, A.; Shazeer, N.; Parmar, N.; Uszkoreit, J.; Jones, L.; Gomez, A. N.; Kaiser, Ł.; and Polosukhin, I. 2017. Attention is all you need. In *NIPS*, volume 30.
- Vinyals, O.; Blundell, C.; Lillicrap, T.; Wierstra, D.; et al. 2016. Matching networks for one shot learning. In *NIPS*, volume 29.
- Wang, L.; Xiong, Y.; Wang, Z.; Qiao, Y.; Lin, D.; Tang, X.; and Gool, L. V. 2016. Temporal segment networks: Towards good practices for deep action recognition. In *ECCV*, 20–36.
- Wang, M.; Xing, J.; and Liu, Y. 2021. Actionclip: A new paradigm for video action recognition. *arXiv preprint arXiv:2109.08472*.
- Wang, X.; Zhang, S.; Qing, Z.; Tang, M.; Zuo, Z.; Gao, C.; Jin, R.; and Sang, N. 2022. Hybrid Relation Guided Set Matching for Few-shot Action Recognition. In *CVPR*, 19948–19957.
- Wu, J.; Zhang, T.; Zhang, Z.; Wu, F.; and Zhang, Y. 2022. Motion-Modulated Temporal Fragment Alignment Network for Few-Shot Action Recognition. In *CVPR*, 9151–9160.
- Yang, L.; Li, L.; Zhang, Z.; Zhou, X.; Zhou, E.; and Liu, Y. 2020. Dpgn: Distribution propagation graph network for few-shot learning. In *CVPR*, 13390–13399.
- Ye, H.-J.; Hu, H.; Zhan, D.-C.; and Sha, F. 2020. Few-shot learning via embedding adaptation with set-to-set functions. In *CVPR*, 8808–8817.
- Yoon, S. W.; Seo, J.; and Moon, J. 2019. Tapnet: Neural network augmented with task-adaptive projection for few-shot learning. In *ICML*, 7115–7123.
- Zhang, B.; Li, X.; Ye, Y.; Huang, Z.; and Zhang, L. 2021. Prototype completion with primitive knowledge for few-shot learning. In *CVPR*, 3754–3762.
- Zhang, H.; Zhang, L.; Qi, X.; Li, H.; Torr, P. H.; and Koniusz, P. 2020a. Few-shot action recognition with permutation-invariant attention. In *ECCV*, 525–542.
- Zhang, L.; Chang, X.; Liu, J.; Luo, M.; Prakash, M.; and Hauptmann, A. G. 2020b. Few-shot activity recognition with cross-modal memory network. *PR*, 108: 107348.
- Zhang, S.; Zhou, J.; and He, X. 2021. Learning implicit temporal alignment for few-shot video classification. In *IJCAI*.
- Zhu, L.; and Yang, Y. 2018. Compound memory networks for few-shot video classification. In *ECCV*, 751–766.
- Zhu, X.; Toisoul, A.; Perez-Rua, J.-M.; Zhang, L.; Martinez, B.; and Xiang, T. 2021. Few-shot action recognition with prototype-centered attentive learning. In *BMVC*.